Vítor Monteiro, Tiago J. C. Sousa, Júlio S. Martins, M. J. Sepúlveda, Carlos Couto, João L. Afonso

"Sliding Mode Control of an Innovative Single-Switch Three-Level Active Rectifier"

IEEE SEST International Conference on Smart Energy Systems and Technologies, Porto, Portugal, Sept. 2019.

Vítor Monteiro, Tiago J. C. Sousa, Júlio S. Martins, M. J. Sepúlveda, Carlos Couto, João L. Afonso, "Sliding Mode Control of an Innovative Single-Switch Three-Level Active Rectifier", IEEE SEST International Conference on Smart Energy Systems and Technologies, Porto, Portugal, Sept. 2019.

Sliding Mode Control of an Innovative Single-Switch Three-Level Active Rectifier

Vítor Monteiro
Industrial Electronics Department
ALGORITMI Research Centre
University of Minho
Campus de Azurem, Portugal
vmonteiro@dei.uminho.pt

Tiago J. C. Sousa
Industrial Electronics Department
ALGORITMI Research Centre
University of Minho
Campus de Azurem, Portugal
tsousa@dei.uminho.pt

Julio S. Martins
Industrial Electronics Department
ALGORITMI Research Centre
University of Minho
Campus de Azurem, Portugal
jmartins@dei.uminho.pt

M. J. Sepulveda
Industrial Electronics Department
ALGORITMI Research Centre
University of Minho
Campus de Azurem, Portugal
mjs@dei.uminho.pt

Carlos Couto
Industrial Electronics Department
ALGORITMI Research Centre
University of Minho
Campus de Azurem, Portugal
ccouto@dei.uminho.pt

Joao L. Afonso
Industrial Electronics Department
ALGORITMI Research Centre
University of Minho
Campus de Azurem, Portugal
jla@dei.uminho.pt

***Abstract*—This paper presents the sliding mode control (SMC) applied to an innovative active rectifier. This proposed active rectifier is constituted by a single-switch, and operates with three voltage levels, evidencing a set of advantages when compared with conventional approaches of power factor correction topologies. Taking into account the diversity of applications for this type of power converter, the SMC is used in order to obtain a robust current tracking. Since the active rectifier is controlled according to the ac grid-side current, the error between such current and its reference is determined, and by employing the SMC, this error is minimized during each sampling period with the objective of selecting the state of the single-switch. A comprehensive description about the SMC implementation, supported by the overall operation of the active rectifier, is presented throughout the paper. The obtained computational results for a set of different operating conditions, comprising significant power ranges and sudden variations, confirm the accurate application of the SMC when applied to the proposed single-switch three-level active rectifier. A comparison is also established with other current control, allowing to confirm the precise application of the SMC strategy.**

Keywords—Active Rectifier; Power Quality; Sliding Mode Control; Smart Grids; Three-Level.

I. INTRODUCTION

Nowadays, the paradigm of smart grids is imposing new technologies to deal with sustainability and environmental issues. As example, the shift to electric mobility is recognized as essential to mitigate the greenhouse gases emissions [1], as well as the on-grid or off-grid integration of renewables [2][3]. Besides, for an effective contribution for improving the energy efficiency, the preservation of power quality aspects is fundamental for the operation of these valences [4][5].

In this sense, from the grid-side point of view, the converters that operate with low harmonic distortion and high power factor are distinct from conventional diode-bridge and multiple-pulse converters [6][7][8]. Notwithstanding the topology, when it is possible to control the current on the grid-side to improve these aspects of power quality, the converters are classified as belonging to the family of active rectifiers, more specifically as power-factor-correction (PFC) converters [6][9]. Interesting and detailed summaries of active rectifiers dedicated to single-phase and three-phase topologies are accessible in [10][11][12][13]. Regardless of the application, when a unidirectional PFC converter is desired, the most used topology is based on a passive diode converter immediately followed by an active converter, with current control at the input-side. Typically, it is used a boost-type converter [14]. The boost converter is the most interesting and simplest to control in PFC structures, because the inductor is in the input-side of the converter and is precisely the current in the inductor that is controlled. A comparative appreciation of PFC structures using only boost-type converters is proven in [15]. However, other ac-dc active converters can be used for PFC structures, as can be found, e.g., in [16] and [17]. More particular are the interleaved PFC structures, where the same ac-dc passive converter is used, but on the dc-side two or more dc-dc active converters are used. The principle of operation is very similar to the solution with only one dc-dc converter, but, in this case, the dc-dc converters, operating with the same current control, are controlled with an interleaved modulation [18]. In addition to the outstanding PFC variants, the multilevel converters can also be used in PFC structures, allowing to optimize the converter in terms of passive filters and voltage stress in the semiconductors [19].

Based on the analysis of the existing PFC structures, this paper discusses a new control strategy applied to an innovative single-switch three-level active rectifier. This converter was initially proposed in [20] for electric mobility applications, but can be used whenever it is necessary to control the current on the grid-side. This converter is composed of a passive ac-dc converter (diodes D_1, D_2, D_3, D_4), which interfaces directly the grid-side and the dc-side, and a bipolar and bidirectional cell (diodes D_5, D_6, D_7, D_8 and IGBT *sw*), which is connected between the phase and the neutral on the grid-side. Apparently, this structure is more complex than the solution based on the ac-dc converter with the boost converter, however, as presented in Section II, this converter has more attractive benefits. A structure, also with a single controlled semiconductor, is presented in [21], but it requires a split dc-link and operates with a double-voltage characteristic on the dc-link. Structures using only a single controlled semiconductor are presented in [15] and [22], but only a high power factor can be obtained, where the current is not accurately sinusoidal.

978-1-7281-1156-8/19/$31.00 ©2019 IEEE

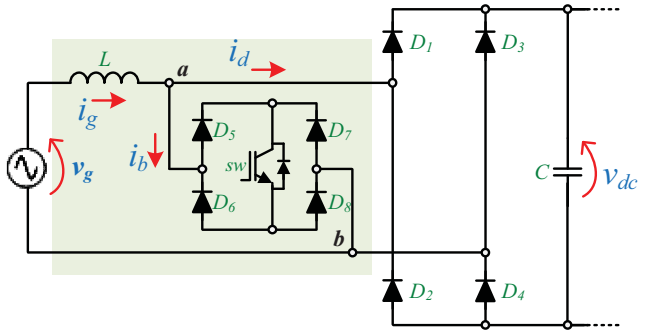

(a)

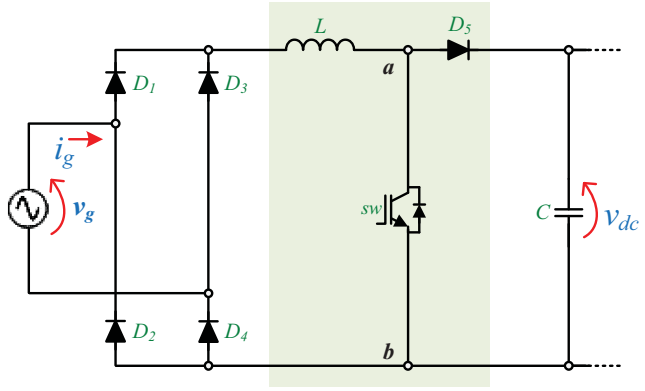

(b)

Fig. 1. Active rectifiers: (a) Proposed single-switch three-level under analysis; (b) Conventional PFC using a dc-dc boost converter.

Nowadays, in power electronics, when it is necessary to control a certain variable, the solution is to use digital controllers instead of analog controllers. In this sense, several controllers can be used, with special emphasis on proportional integral (PI) and proportional integral derivative (PID) controllers. Although these controllers are widely used and present good results, there are alternatives that present better results when applied to control certain variables, depending on the power electronics converter. Often, the major problems with the use of controllers of this type in power electronics are resonance phenomena. In this sense, as an alternative to these controllers for power electronics applications, stands out the control in sliding mode [23]. As shown in [24] and [25], the control in sliding mode can be applied in power electronics converters in continuous and discontinuous operation mode, respectively. In [26] a fairly comprehensive approach to this type of control is presented when applied to the most basic dc-dc converters (buck, boost, buck-boost), where experimental results of the boost converter are presented. When applied to the boost PFC, this type of controller can be used for controlling the output voltage or the input current [27]. As shown in [28] and [29], this type of controller is also quite robust when applied to ac-dc converters of PFC structures.

In the scope of this paper, a control based on sliding mode control (SMC) is presented for the three-level single-switch active rectifier, aiming to control the grid-side current for any reference current. Moreover, a comparative analysis with the existing predictive control (finite control set) for the same active rectifier is also established. Based on the addressed subject, the paper is organized as follows. Section II presents a theoretical analysis of the active rectifier, supported by a comparative analysis with the conventional approach of PFC structure; Section III introduces the implementation of the SMC for the active rectifier under analysis; Section IV shows and discusses the obtained results in steady- and transient-state; Finally, Section V ends the paper with the conclusions.

II. Theoretical Analysis of the Proposed Three-Level Single-Switch Active Rectifier

The topology of the single-switch three-level active rectifier is presented in Fig. 1(a), and the topology of the conventional PFC with the dc-dc boost converter is presented in Fig. 1(b). By applying a proper current control algorithm and modulation, internally to the topology, the grid-side current (i_g) is divided in two currents: i_d and i_b. The current in the main diode bridge (i_d) is associated with the voltage levels v_{dc} and $-v_{dc}$ (voltage between a and b when the IGBT is off) and the current in the bipolar and bidirectional cell (i_b) is associated with the voltage level 0 (when the IGBT is on). Comparing with the conventional PFC with the diode bridge and the boost converter (Fig. 1(b)), the rms value of the current in the main diode bridge (diodes D_1, D_2, D_3, and D_4 represented in both figures) is reduced. Globally, the single-switch three-level active rectifier requires more three diodes (diodes D_5, D_6, D_7, and D_8 for the bipolar and bidirectional cell comparing with the diode D_5 of the boost converter), which is a drawback in terms of required components. Nevertheless, in counterpart, it has more advantages in terms of energy efficiency. Comparing both topologies when the IGBT is on, in both cases are used two diodes for obtaining the level 0 in both positive and negative half-cycles. On the other hand, comparing both topologies when the IGBT is off, the single-switch three-level active rectifier uses two diodes, while the conventional PFC requires an additional diode (the diode D_5 of the boost converter). Therefore, it is possible to improve the energy efficiency when using the single-switch three-level active rectifier. An exhaustive comparison between the topologies is out of the scope of this paper, however, a complete comparison based on an experimental validation is presented in [20]. Since the single-switch three-level active rectifier is a more interesting topology for the same purpose, the focus of this paper is to analyze the application of the SMC to this topology in detriment of other classical current control algorithms.

III. Sliding Mode Control of the Proposed Three-Level Single-Switch Active Rectifier

Fig. 1(a) shows the topology of the single-switch three-level active rectifier, where the grid-side current (i_g) is the variable that is intent to control using the SMC, as following described.The operation of the topology is function of the controlling variable u, which defines the state of the IGBT *sw*. When it is equal to 1, means that the IGBT is on and when it is 0, means that the IGBT is off. This variable establishes the control law expressed by:

$$u = \begin{cases} 1 & ,S > 0 \\ 0 & ,S < 0 \end{cases}, \tag{1}$$

where S is the instantaneous value of the control trajectory, which is defined by:

$$S = \alpha_1 x_1 + \alpha_2 x_2 = [\alpha_1 \quad \alpha_2] \begin{bmatrix} x_1 \\ x_2 \end{bmatrix}, \tag{2}$$

where α_1 and α_2 are identified as sliding coefficients, x_1 and x_2 are control equations, x_1 defines the error between the

reference of current (i_g*) and the current (i_g) and x_2 defines the integral of the error (defined between i_g* and i_g). Therefore, based on this analysis, equations x_1 and x_2 can be written as:

$$\begin{bmatrix} x_1 \\ x_2 \end{bmatrix} = \begin{bmatrix} i_g{}^* - i_g \\ \int (i_g{}^* - i_g) dt \end{bmatrix} = \begin{bmatrix} x_1 \\ \int x_1 dt \end{bmatrix}. \quad (3)$$

Analyzing the topology in more detail in terms of the variables, mainly knowing that i_g is the current in the inductor L, the equation x_1 can be expressed by:

$$x_1 = i_g{}^* - i_g = i_g{}^* - \frac{1}{L}\int v_L \, dt \,, \quad (4)$$

where v_L, according to the voltage assumed by the converter, is defined as a function of the variable u, by:

$$v_L = v_g - (1-u)v_{dc} \,. \quad (5)$$

Thus, using these previous equations, equation (3) can be rewritten as:

$$\begin{bmatrix} x_1 \\ x_2 \end{bmatrix} = \begin{bmatrix} i_g{}^* - \frac{1}{L}\int (v_g - u v_{dc}) \, dt \\ \int x_1 dt \end{bmatrix}. \quad (6)$$

In order to guarantee the operation in sliding mode, the following condition must be guaranteed:

$$\lim_{S \to 0} S\dot{S} < 0 \,, \quad (7)$$

where $\dot{S}$ is the derivative of S. According to this condition, there are two cases of analysis: when $S \to 0^+$ and when $S \to 0^-$. For the first case ($S \to 0^+$), it can be written that:

$$\dot{S} < 0 \Leftrightarrow \alpha_1 \frac{dx_1}{dt} + \alpha_2 \frac{dx_2}{dt} < 0 \,. \quad (8)$$

By making $u = 0$ (meaning that the IGBT is off), the state equation can be expressed by:

$$\begin{bmatrix} \dot{x_1} \\ \dot{x_2} \end{bmatrix} = \begin{bmatrix} \frac{di_g{}^*}{dt} - \frac{1}{L}(v_g - v_{dc}) \\ i_g{}^* - i_g \end{bmatrix}, \quad (9)$$

thus, obtaining:

$$\alpha_1 \left(\frac{di_g{}^*}{dt} - \frac{1}{L}(v_g - v_{dc}) \right) + \alpha_2 (i_g{}^* - i_g) < 0 \,, \quad (10)$$

which can be simplified to:

$$\alpha_1 \left(\frac{di_g{}^*}{dt} - \frac{1}{L} v_g \right) + \alpha_1 \frac{1}{L} v_{dc} + \alpha_2 (i_g{}^* - i_g) < 0 \,, \quad (11)$$

resulting in the equation, for this case, established by:

$$\alpha_1 \left(\frac{di_g{}^*}{dt} - \frac{1}{L} v_g \right) + \alpha_2 (i_g{}^* - i_g) < \alpha_1 \frac{1}{L} v_{dc} \,. \quad (12)$$

For the second case ($S \to 0^-$), it can be written that:

$$\dot{S} > 0 \Leftrightarrow \alpha_1 \frac{dx_1}{dt} + \alpha_2 \frac{dx_2}{dt} > 0 \,. \quad (13)$$

By making $u = 1$ (meaning that the IGBT is on), the state equation can be expressed by:

$$\begin{bmatrix} \dot{x_1} \\ \dot{x_2} \end{bmatrix} = \begin{bmatrix} \frac{di_g{}^*}{dt} - \frac{1}{L} v_g \\ i_g{}^* - i_g \end{bmatrix}, \quad (14)$$

resulting in the equation, for this case, established by:

$$\alpha_1 \left(\frac{di_g{}^*}{dt} - \frac{1}{L} v_g \right) + \alpha_2 (i_g{}^* - i_g) > 0 \,. \quad (15)$$

By combining the two expressions resulting from the two cases, it is obtained:

$$0 < \alpha_1 \left(\frac{di_g{}^*}{dt} - \frac{1}{L} v_g \right) + \alpha_2 (i_g{}^* - i_g) < \alpha_1 \frac{1}{L} v_{dc} \,. \quad (16)$$

Multiplying both terms of the previous equation by L/α_1, equation (16) can be rewritten by:

$$0 < L \left(\frac{di_g{}^*}{dt} - \frac{1}{L} v_g \right) + L \frac{\alpha_2}{\alpha_1} (i_g{}^* - i_g) < v_{dc} \,, \quad (17)$$

resulting in the control equation established by:

$$0 < L \frac{di_g{}^*}{dt} - v_g + L \frac{\alpha_2}{\alpha_1} (i_g{}^* - i_g) < v_{dc} \,. \quad (18)$$

Equation (18) establishes a reference voltage, which is compared to a carrier of amplitude v_{dc} in order to obtain a voltage (voltage v_{ab} between points a and b in Fig. 1(a)) that produces the desired current (i.e., the current i_g follows its reference i_g*). However, for the implementation of equation (18), it is necessary to know the sliding coefficients. These can be determined by making $S = 0$, resulting in:

$$S = \alpha_1 x_1 + \alpha_2 x_2 = 0 \,. \quad (19)$$

Deriving the equation (19) in order to time, it is obtained:

$$\alpha_1 \frac{dx_1}{dt} + \alpha_2 x_1 = 0 \,, \quad (20)$$

which can be simplified to:

$$\frac{dx_1}{dt} + \frac{\alpha_2}{\alpha_1} x_1 = 0 \,. \quad (21)$$

Since equation (21) is of the type:

$$\frac{dx}{dt} + kx = 0 \,, \quad (22)$$

the solution is expressed by:

$$x(t) = C \, e^{-\frac{t}{T_s}} \,, \quad (23)$$

where C is determined as a function of the initial conditions and T_s is the time constant, defined as a function of the sampling frequency, by:

$$T_s = \frac{1}{f_s} \,. \quad (24)$$

Thus, the sliding coefficients are defined by:

$$\frac{\alpha_2}{\alpha_1}=\frac{1}{T_s}=f_s. \quad (25)$$

IV. SMC Applied to the Proposed Single-Switch Three-Level Active Rectifier: Analysis and Validation

The validation of the SMC applied to the single-switch three-level active rectifier was performed following the specifications listed in Table I and with the PSIM software. The different rms values assumed by the reference current were considered taking into account the operating power on the dc-side of the topology, where any type of dc-dc converter can be associated. It is not an objective of this paper to deal with any particular power theory responsible for establishing the reference of current, and therefore, a simple control strategy based on the Fryze-Buchholz-Depenbrock (FBD) power theory was used.

TABLE I
Characteristics of the Simulation Model

Parameter	Value
Grid Voltage (V)	230
Grid Frequency (Hz)	50
Maximum Grid Voltage THD (%)	4
Maximum Power (kW)	6.5
Grid Current @ Full Power THD (%)	2
Total Power Factor @ Full Power	0.99
Dc-link Voltage (V)	400
Inductor Filter (H)	0.003
Switching Frequency (kHz)	20
Sampling Frequency (kHz)	40

Fig. 2 presents a result that shows the application of the SMC to control the ac grid-side current (i_g) in steady-state, and considering two different situations of operation. Initially, in case #1, it is assumed that the ac grid-side voltage is purely sinusoidal, without any kind of disturbance of power quality, and that the waveform of the reference current is based on this voltage, therefore also purely sinusoidal (only affected, proportionally, in the amplitude). As it turns out, due to the application of the SMC, the controlled grid-side current (i_g) is sinusoidal. Subsequently, in case #2, it is considered a situation where the grid-side voltage has harmonic distortion, in this case with a value of total harmonic distortion (THD) of 3.93% (this value was assumed considering a real measure of voltage of an electrical installation). In addition, in this case #2, it is assumed that the reference current is directly proportional to the grid-side voltage, also presenting a THD value of 3.93%. It is important to mention that this situation is not the most beneficial from the point of view of controllability of the topology, however it was considered as an extreme situation, in which the reference current may not be sinusoidal, allowing to validate the applicability of the SMC to the topology. Even considering this scenario of a reference current (i_g*) with harmonic distortion, it is verified that the grid-side current (i_g) is properly controlled according to i_g*, proving the applicability of the SMC for controlling the topology. In this Fig. 2, it is also possible to verify the internal currents within the topology, namely the current in the main diode bridge (i_d) and the current in the bipolar and bidirectional cell (i_b). As described in Section II, the current on the grid-side (i_g) corresponds to the sum of the current i_d

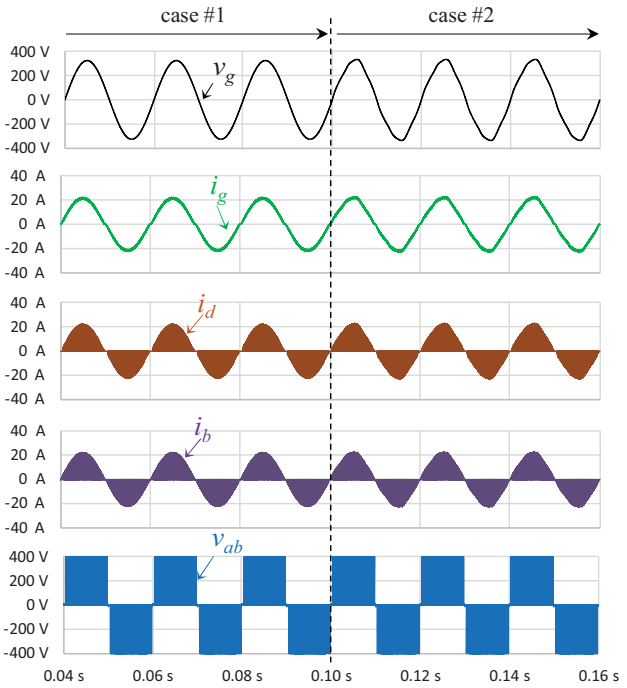

Fig. 2. Validation in steady-state of the grid-side current (i_g), internal currents in the topology (i_d, i_b), and produced voltage (v_{ab}) considering: Case #1 with sinusoidal grid-side voltage (v_g) and sinusoidal reference current; Case #2 with distorted grid-side voltage (v_g) and distorted reference current.

(when the IGBT is off and v_{ab} assumes the value of v_{dc} or -v_{dc}) with the current i_b (when the IGBT is on and v_{ab} assumes the value 0). As it turns out, the converter assumes the three possible voltage levels, thus proving one of the main characteristics of the topology.

Fig. 3 shows a result considering the control of the grid-side current (i_g) in transient-state. Firstly, in order to obtain the most realistic result possible, a sinusoidal reference current (i_g*) was considered, notwithstanding the distortion of the grid-side voltage (v_g). In this figure, the same variables can be visualized as in the Fig. 2, but two distinct transient moments were considered. In case #1, the operation is the same as in the previous case. In Fig. 3(b), it is possible to verify in detail the grid-side current (i_g) when compared with its reference (i_g*). When t = 0.165 s, a change in the reference current to the double occurs, giving rise to case #2 of operation. Despite the instantaneous change of the reference current, the controlled current (i_g) reaches the reference (i_g*) in a reduced time interval, more precisely in about 0.25 ms, which is a quite acceptable time taking into account the sudden change and that it is an active rectifier. From Fig. 3(a), a zoom showing in detail a comparison of both variables during the transient-state is presented in Fig. 3(c). As it should be, the i_d and i_b currents change proportionally according to the current i_g. Moreover, the voltage assumed by the topology (v_{ab}) maintains the three levels of operation, independently of the transient-state operation. Subsequently, when t = 0.195 s, the reference current changes again instantaneously, but, in this case, to half of the previous value and considering the change in the negative half-cycle, giving rise to case #3 of operation. Similar to the previous case, the detail of the comparison between the current (i_g) with its reference (i_g*) is shown in Fig. 3(d). Also in this case, despite the instantaneous change of the reference current, the controlled current (i_g) reaches that reference (i_g*) in a reduced time interval, more precisely

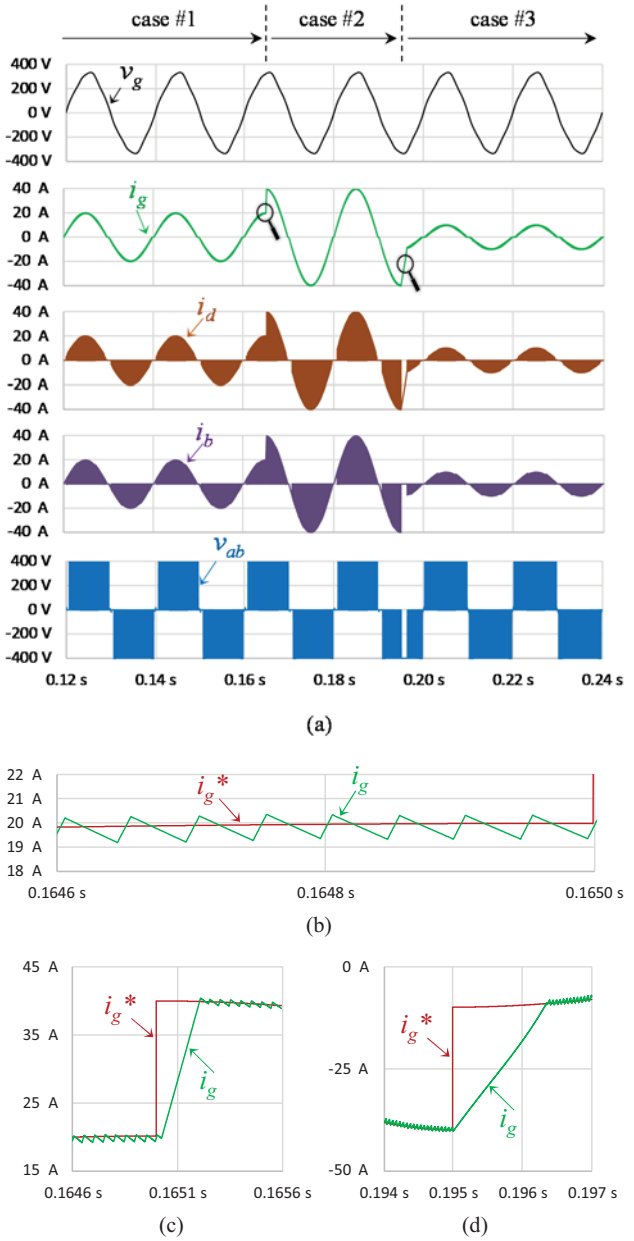

Fig. 3. Validation in transient-state: (a) Grid-side current (i_g), internal currents in the topology (i_d, i_b), and produced voltage (v_{ab}); (b) Detail of the grid-side current (i_g) compared with its reference (i_g*); (c) Detail of the grid-side current (i_g) compared with its reference (i_g*) during the increase of the reference; (d) Detail of the grid-side current (i_g) compared with its reference (i_g*) during the decrease of the reference.

in about 1.3 ms. Also this value is quite acceptable considering the change made and that it is a topology of active rectifier. As it turns out, this situation, where the reference current is reduced, is more critical, but even so, the current follows its reference satisfactorily. Similarly to the previous case, it is also verified that the currents i_d and i_b decrease proportionally with i_g and that the converter continues to operate with the three voltage levels.

In order to verify the advantages of the SMC applied to the single-switch three-level topology, a comparison was made with another current control strategy, namely with finite-control-set model-predictive-control (as originally presented in [20]). The comparison was performed considering the same topology, the same specifications listed in Table I, but for both current control strategies. The results of this comparison are presented in Fig. 4, where the same reference current (i_g*) was considered for both control

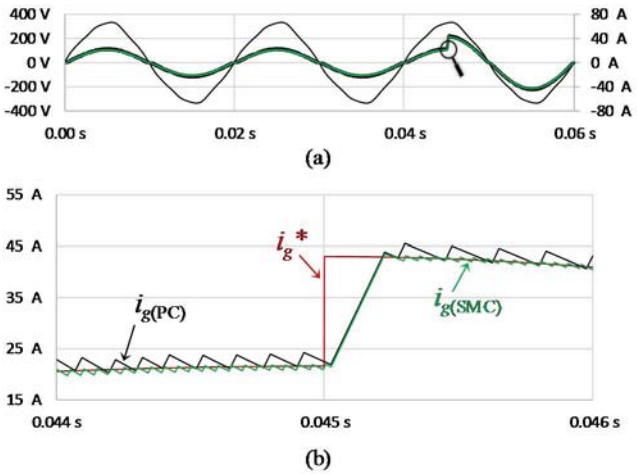

Fig. 4. Validation of the SMC compared with the predictive control in transient-state: (a) Grid-side currents ($i_{g(SMC)}$, $i_{g(PC)}$) and grid-side voltage (v_g); (b) Detail of the grid-side currents ($i_{g(SMC)}$, $i_{g(PC)}$) compared with the reference (i_g*).

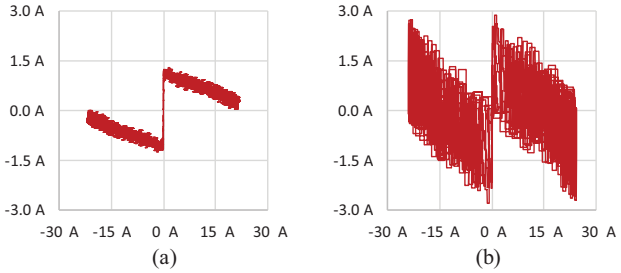

Fig. 5. Validation of the grid-side currents ($i_{g(SMC)}$, $i_{g(PC)}$) in function of the error (between the reference and the measured currents) when applying: (a) The SMC control; (b) The predictive control.

strategies (a sinusoidal reference with a distorted grid voltage). As it turns out, when using the SMC strategy, the grid-side current follows its reference more effectively, presenting a smaller ripple of current. To verify more in detail a comparison of both strategies, a transient-state was considered. Therefore, in Fig. 4(b) both currents, resultant from the application of both current control strategies, are presented in detail when compared with the same reference. From this result, it can be verified that, clearly, the SMC strategy is more interesting when applied to the single-switch three-level active rectifier. Although they present similar times until reaching the new value of reference, the ripple of current, resultant from the application of the SMC, is always smaller. In addition, based on the comparison of both current control strategies, in Fig. 5, the relationship between the current i_g and the current error (difference between reference of current and measured current) is shown in steady-state. As it turns out, the SMC is the strategy that presents best results, although presenting a slightly more significant error in the crossing by zero.

V. Conclusions

This paper introduces the sliding mode control (SMC) when applied to an innovative single-switch three-level active rectifier. The advantages of this proposed active rectifier, as well as a comparison with a conventional solution (based on a dc-dc boost converter) are presented. Thus, throughout the paper, the details of implementing the SMC strategy are minutely defined when applied to control the ac grid-side current of the proposed active rectifier. The validation was verified for various operating conditions, namely considering different reference current waveforms

(sinusoidal and with harmonic distortion), and also considering instantaneous changes of the reference current (to the double and half of the initial value). The validation was also verified by comparing, in steady-state and transient-state, the SMC strategy with a predictive strategy, allowing to confirm the precise application of the SMC when applied to the proposed single-switch three-level active rectifier. Summarizing, the superiority of the proposed innovative active rectifier was verified in this paper, especially when controlled with the SMC strategy.

ACKNOWLEDGMENT

This work has been supported by FCT – Fundação para a Ciência e Tecnologia within the Project Scope: UID/CEC/00319/2019. This work has been supported by FCT Project *newERA4GRIDs* PTDC/EEI-EEE/30283/2017, and by the FCT Project *DAIPESEV* PTDC/EEI-EEE/30382/2017. Tiago Sousa is supported by the doctoral scholarship SFRH/BD/134353/2017 granted by FCT.

REFERENCES

[1] Vítor Monteiro, Bruno Exposto, João C. Ferreira, João L. Afonso, "Improved Vehicle-to-Home (iV2H) Operation Mode: Experimental Analysis of the Electric Vehicle as Off-Line UPS," IEEE Transactions on Smart Grid, vol.8, no.6, pp.2702-2711, Nov. 2017.

[2] Shuang Gao, K. T. Chau, Chunhua Liu, Diyun Wu, C. C. Chan, "Integrated Energy Management of Plug-in Electric Vehicles in Power Grid With Renewables," IEEE Trans. Veh. Technol., vol.63, no.7, pp.3019-3027, Sept. 2014.

[3] Vitor Monteiro, João C. Ferreira, Andres A. Nogueiras Melendez, Carlos Couto, João L. Afonso, "Experimental Validation of a Novel Architecture Based on a Dual-Stage Converter for Off-Board Fast Battery Chargers of Electric Vehicles," IEEE Trans. Veh. Tech., vol.67, no.2, pp.1000-1011, Feb. 2018.

[4] Vítor Monteiro, João Paulo Carmo, J. G. Pinto, João L. Afonso, "A Flexible Infrastructure for Dynamic Power Control of Electric Vehicle Battery Chargers," IEEE Trans. Veh. Technol., vol.65, no.6, pp.4535-4547, June 2016.

[5] Vítor Monteiro, Henrique Gonçalves, João L. Afonso, "Impact of Electric Vehicles on Power Quality in a Smart Grid Context," IEEE EPQU International Conference on Electrical Power Quality and Utilisation, pp.1-6, Oct. 2011.

[6] Bhim Singh, Brij N. Singh, Ambrish Chandra, Kamal Al-Haddad, Ashish Pandey, Dwarka P. Kothari, "A Review of Single-Phase Improved Power Quality AC-DC Converters," IEEE Trans. Ind. Electron., vol.50, no.5, pp.962-981, Oct. 2003.

[7] Vítor Monteiro, Bruno Exposto, J. G. Pinto, M. J. Sepúlveda, Andrés A. Nogueiras Meléndez, João L. Afonso, "Three-Phase Three-Level Current-Source Converter for EVs Fast Battery Charging Systems," IEEE ICIT International Conference on Industrial Technology, Seville Spain, pp.1401-1406, March 2015.

[8] Vítor Monteiro, J. G. Pinto, Bruno Exposto, João L. Afonso, "Comprehensive Comparison of a Current-Source and a Voltage-Source Converter for Three-Phase EV Fast Battery Chargers," CPE International Conference on Compatibility and Power Electronics, Lisboa Portugal, pp.173-178, June 2015.

[9] Oscar García, José A. Cobos, Roberto Prieto, Pedro Alou, Javier Uceda, "Single Phase Power Factor Correction: A Survey," IEEE Trans. Power Electron., vol.18, no.3, pp.749-755, May 2003.

[10] Bhim Singh, Brij N. Singh, Ambrish Chandra, Kamal Al-Haddad, Ashish Pandey, Dwarka P. Kothari, "A Review of Single-Phase Improved Power Quality AC-DC Converters," IEEE Trans. Ind. Electron., vol.50, no.5, pp.962-981, Oct. 2003.

[11] Bhim Singh, Brij N. Singh, Ambrish Chandra, Kamal Al-Haddad, Ashish Pandey, Dwarka P. Kothari, "A Review of Three-Phase Improved Power Quality AC-DC Converters," IEEE Trans. Ind. Electron., vol.51, no.3, pp.641-660, June 2004.

[12] Johann W. Kolar, Thomas Friedli, "The Essence of Three-Phase PFC Rectifier Systems—Part I," IEEE Trans. Power Electron., vol.28, no.1, pp.176-198, Jan. 2013.

[13] Thomas Friedli, Michael Hartmann, Johann W. Kolar, "The Essence of Three-Phase PFC Rectifier Systems—Part II," IEEE Trans. Power Electron., vol.29, no.2, pp.543-560, Feb. 2014.

[14] João Paulo M. Figueiredo, Fernando L. Tofoli, Bruno Leonardo A. Silva, "A Review of Single-Phase PFC Topologies Based on The Boost Converter," IEEE INDUSCON International Conference on Industry Applications, pp.1-6, Nov. 2010.

[15] Fariborz Musavi, Murray Edington, Wilson Eberle, William G. Dunford, "Evaluation and Efficiency Comparison of Front End AC-DC Plug-in Hybrid Charger Topologies," IEEE Trans. Smart Grid, vol.3, no.1, pp.413-421, Mar. 2012.

[16] José Rodríguez, Jih-Sheng Lai, Fang Zheng Peng, "Multilevel Inverters: A Survey of Topologies, Controls, and Applications," IEEE Trans. Ind. Electron., vol.49, no.4, pp.724-738, Aug. 2002.

[17] Jih-Sheng Lai, Fang Zheng Peng, "Multilevel Converters-A New Breed of Power Converters," IEEE Trans. Ind. Appl., vol.32, no.3, pp.509-517, May 1996.

[18] Laszlo Huber, Yungtaek Jang, Milan Jovanovic, "Performance Evaluation of Bridgeless PFC Boost Rectifier," IEEE Trans. Power Electron., vol.23, no.3, pp.1381-1390, May 2008.

[19] Jong-Jae Lee, Jung-Min Kwon, Eung-Ho Kim,Woo-Young Choi, Bong-Hwan Kwon, "Single-Stage Single-Switch PFC Flyback Converter Using a Synchronous Rectifier," IEEE Trans. Ind. Electron., vol.55, no.3, pp.1352-1365, Mar. 2008.

[20] Vítor Monteiro, Andrés A. Nogueiras Meléndez, Carlos Couto, João L. Afonso, "Model Predictive Current Control of a Proposed Single-Switch Three-Level Active Rectifier Applied to EV Battery Chargers," IEEE IECON Industrial Electronics Conference, Florence Italy, pp.1365-1370, Oct. 2016.

[21] André De Bastiani Lange, Thiago Batista Soeiro, Márcio Silveira Ortmann, Marcelo Lobo Heldwein, "Three-Level Single-Phase Bridgeless PFC Rectifiers," IEEE Trans. Power Electron., vol.30, no.6, pp.2935-2949, June 2015.

[22] Vítor Monteiro, Andrés A. Nogueiras Meléndez, João C. Ferreira, Carlos Couto, João L. Afonso, "Experimental Validation of a Proposed Single-Phase Five-Level Active Rectifier Operating with Model Predictive Current Control," IEEE IECON Industrial Electronics Conference, pp.3939-3944, Nov. 2015.

[23] Asif Sabanovic, Karel Jezernik, Nadira Sabanovic, "Sliding Modes Applications in Power Electronics and Electrical Drives," Springer Variable Structure Systems: Towards the 21st Century, pp.223□251, 2002.

[24] Siew-Chong Tan, Y. M. Lai, C. K. Tse, "Design of PWM Based Sliding Mode Voltage Controller for DC-DC Converters Operating in Continuous Conduction Mode," European Conference on Power Electronics and Applications, pp.1-10, Sept. 2006.

[25] Siew-Chong Tan, Y. M. Lai, Chi K. Tse, Luis Martinez-Salamero, Angel Cid-Pastor, "Design of Pulse width-Modulation Based Sliding Mode Controllers for Power Converters in Discontinuous Conduction Mode," IEEE IECON Conference on Industrial Electronics, pp.2769-2774, Nov. 2006.

[26] Siew-Chong Tan, Y. M. Lai, Chi K. Tse, "A Unified Approach to the Design of PWM-Based Sliding-Mode Voltage Controllers for Basic DC-DC Converters in Continuous Conduction Mode," IEEE Transactions on Circuits and Systems – I, vol.53, no.8, pp.1816-1827, Aug. 2006.

[27] Siew-Chong Tan, Y. M. Lai, C. K. Tse, Chi Kin Wu, "A Pulsewidth Modulation Based Integral Sliding Mode Current Controller for Boost Converters," IEEE PESC Power Electronics Specialists Conference, pp.1-7, June 2006.

[28] Abdelhalim Kessal, Lazhar Rahmani, "Analysis and design of sliding mode controller gains for boost power factor corrector," ISA Transactions, pp.638-643, 2013.

[29] G. Chu, Siew-Chong Tan, C. K. Tse, Siu Chung Wong, "General Control for Boost PFC Converter from a Sliding Mode Viewpoint," IEEE PESC Power Electronics Specialists Conference, pp.4452-4456, June 2008.